

# Enhancement of the electron electric dipole moment in gadolinium garnets

T. N. Mukhamedjanov, V. A. Dzuba, O. P. Sushkov  
*School of Physics, University of New South Wales,  
Sydney 2052, Australia*

Effects caused by the electron electric dipole moment (EDM) in gadolinium garnets are considered. Experimental studies of these effects could improve current upper limit on the electron EDM by several orders of magnitude. We suggest a consistent theoretical model and perform calculations of observable effects in gadolinium gallium garnet and gadolinium iron garnet. Our calculation accounts for both direct and exchange diagrams.

## I. INTRODUCTION

Violation of the combined symmetry of charge conjugation (C) and parity (P) has been discovered in the decay of the  $K^0$  meson about 40 years ago [1]. The exact origin of this symmetry violation remains an enigma, although the so-called standard model of electroweak interactions can describe these processes phenomenologically. It has also been proposed by Sakharov [2] that the matter–antimatter asymmetry observed in our Universe could have arisen from a CP-violating interaction active at an early stage of the Big Bang. The CP-violation implies a time-reversal (T) asymmetry, because there are strong reasons to believe that the combined CPT-symmetry should not be violated [3]. Violation of the time reversal symmetry has been observed recently in decays of K-mesons [4]. T-violation together with well known parity (P) violation (T,P-violation) provides a nonzero electric dipole moment (EDM) of a system in a stationary quantum state. This is why searches for EDM of elementary particles, atoms and molecules are very important for studies of violations of fundamental symmetries [5]. In the present work we concentrate on the electron EDM. The present best limitation on the electron EDM comes from the experiment with an atomic Thallium beam [6],

$$d_e < 1.6 \times 10^{-27} e \cdot \text{cm}. \quad (1)$$

There have been recent suggestions [7, 8] to improve the sensitivity to the electron EDM substantially by working with solids. In particular gadolinium gallium garnet,  $\text{Gd}_3\text{Ga}_5\text{O}_{12}$  (GGG), and gadolinium iron garnet  $\text{Gd}_3\text{Fe}_5\text{O}_{12}$  (GdIG) have been suggested. The idea for searches of the electron EDM in solid state experiments was first suggested by Shapiro in 1968 [9]. There are two ways to perform such an experiment. The first one is to apply an external magnetic field to the solid. Polarization of electrons by the magnetic field causes alignment of electron EDMs, and hence induces a voltage across the sample that could be detected. Another possibility is to apply a strong external electric field. This would align the EDMs of bound electrons and hence lead to a simultaneous alignment of the electron spins; the magnetic field arising from this alignment could be detected experimentally. An experiment of this kind has been performed with nickel-zinc ferrite [10]. Due to experimental limitations the result was not very impressive. However, according to estimates presented in Refs. [7, 8], application of novel experimental techniques and measurements with GGG and GdIG makes this direction highly promising.

The first calculation of the T,P-odd effects in GGG and GdIG has been performed in Ref. [11] (see also Refs. [12, 13]). The mechanism considered in that work was similar to the mechanism of T,P-violation in atoms due to the T,P-odd nuclear forces [14]. In essence the  $\text{Gd}^{3+}$  ion has been treated as a large nucleus that has some effective Schiff moment. External electrons that belong to  $\text{O}^{2-}$  ions penetrate inside the  $\text{Gd}^{3+}$  ion and interact with the “Schiff moment” of the ion. This results in an effective interaction between the lattice deformation and the electron EDM. It has been also pointed out in Ref. [11] that there is a contribution that can not be reduced to the “Schiff moment mechanism”, this contribution is due to the exchange between external and internal electrons. However the exchange diagrams estimated in Ref. [11] gave a small contribution. In the present work we have found a new class of exchange diagrams that are very important. Calculation of the effect with account of exchange diagrams is not a simple problem because in this case the logic that leads to the Schiff moment [11, 14] is not valid. For the same reason the simplistic model of the electronic structure of Gadolinium garnet used in [11] is not sufficient for the present calculation. Therefore to perform the present calculation we have developed a more accurate model that treats gadolinium and oxygen electrons simultaneously. We believe that the present calculation is more accurate than that performed in Ref. [11]. Nevertheless, surprisingly, the results are very close.

## II. THEORETICAL MODEL FOR ELECTRONIC STRUCTURE

### A. Single-electron effective potential

Compounds of our interest, gadolinium iron garnet and gadolinium gallium garnet, are ionic crystals, consisting of  $\text{Gd}^{3+}$ ,  $\text{Fe}^{3+}$  (or  $\text{Ga}^{3+}$ ) and  $\text{O}^{2-}$  ions. Uncompensated electron spins are localized at  $\text{Gd}^{3+}$  ion, which has a  $4f^7$  configuration, and  $\text{Fe}^{3+}$  ion, whose electronic configuration is  $4d^5$ . Both paramagnetic ions contribute to the T,P-odd effect. However, contribution of the ion to the T,P-odd effect scales as  $Z^3$ , where  $Z$  is the nuclear charge (see, e.g. [5]). Therefore, we neglect the contribution of  $\text{Fe}^{3+}$  and consider only  $\text{Gd}^{3+}$  ions.

To describe an isolated  $\text{Gd}^{3+}$  ion we use the effective potential in the following parametric form

$$V_{\text{Gd}}(\mathbf{r}) = \frac{1}{r} \frac{(Z_i - Z)(e^{-\frac{\mu}{d}} + 1)}{(1 + \eta r)^2 (e^{\frac{r-\mu}{d}} + 1)} - \frac{Z_i}{r}. \quad (2)$$

Here we use atomic units,  $Z$  is charge of the nucleus,  $Z_i$  is charge of the core of the ion, and  $\mu$ ,  $d$  and  $\eta$  are some parameters that describe the core. Solution of the Dirac equation with the potential (2) gives wave functions and energies of electron states. We use the following values of the parameters

$$\mu = 1.00, \quad d = 1.00 \quad \eta = 2.35. \quad (3)$$

These values provide a fit of experimental energy levels for  $\text{Gd}^{3+}$  ( $Z_i = 4$ ) and  $\text{Gd}^{2+}$  ( $Z_i = 3$ ). Calculated and experimental [15] energy levels averaged over fine structure are shown in Table I.

Ion	electron state	Calculation	Experiment
$\text{Gd}^{3+}$	$4f$	-363	-355
	$5d$	-281	
$\text{Gd}^{2+}$	$5d$	-156	-157
	$6s$	-120	-121
	$6p$	-158	-156

TABLE I: Calculated and experimental energy levels with respect to the ionization limit. The levels are averaged over fine structure. Units  $10^3 \text{ cm}^{-1}$ .

### B. Account of $\text{Gd}^{3+}$ environment

In the garnet structure each gadolinium ion is surrounded by eight oxygen ions  $\text{O}^{2-}$  in a dodecahedron configuration (resembles distorted cube), see Ref. [16]. The configuration at two different angles of view is shown in Fig. 1. The

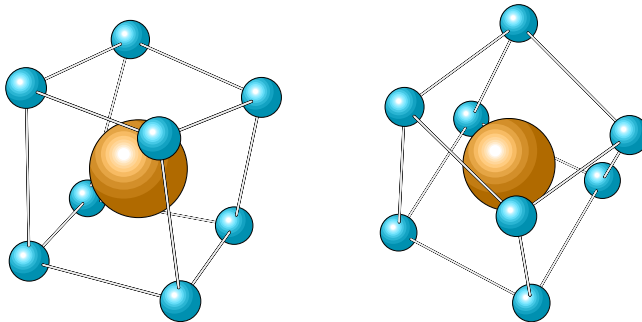


FIG. 1: Dodecahedron configuration of  $\text{O}^{2-}$  ions around  $\text{Gd}^{3+}$  ion in garnet structure.

Gd–O distance is  $r_o = 4.53a_B$ , where  $a_B$  is the Bohr radius. We need to know wave functions of oxygen electrons inside the  $\text{Gd}^{3+}$  ion. Electronic configuration of  $\text{O}^{2-}$  is  $1s^2 2s^2 2p^6$ . Consider  $2p$  orbitals of the ion. It can be shown that  $2p_\pi$  orbitals do not contribute to the effect and we need to consider only  $2p_\sigma$  orbitals, pointing towards  $\text{Gd}^{3+}$ . Every  $2p_\sigma$  orbital is double occupied, so we have 16 electrons in the vicinity of  $\text{Gd}^{3+}$ . In first approximation one can neglect distortion of the oxygen cube and use a linear combination of oxygen  $2p_\sigma$  orbitals with definite symmetry with

respect to the cubic group. We are particularly interested in the  $|S\rangle$  wavefunction, which is symmetric with respect to reflection of cube's main axes, and  $|P_x\rangle$ ,  $|P_y\rangle$  and  $|P_z\rangle$  wavefunctions, which change sign with reflection of  $x$ ,  $y$  and  $z$  axes, correspondingly. They are of the form:

$$\begin{aligned}
 |S\rangle &= \frac{|1\rangle + |2\rangle + |3\rangle + |4\rangle + |5\rangle + |6\rangle + |7\rangle + |8\rangle}{\sqrt{8}}, \\
 |P_x\rangle &= \frac{|1\rangle + |2\rangle - |3\rangle - |4\rangle + |5\rangle + |6\rangle - |7\rangle - |8\rangle}{\sqrt{8}}, \\
 |P_y\rangle &= \frac{|1\rangle - |2\rangle - |3\rangle + |4\rangle + |5\rangle - |6\rangle - |7\rangle + |8\rangle}{\sqrt{8}}, \\
 |P_z\rangle &= \frac{|1\rangle + |2\rangle + |3\rangle + |4\rangle - |5\rangle - |6\rangle - |7\rangle - |8\rangle}{\sqrt{8}}.
 \end{aligned} \tag{4}$$

Here  $|n\rangle$  denotes  $2p_\sigma$  orbital of  $n$ -th oxygen ion as they are enumerated in Fig. 2. There are also three D-wave states and one F-wave state combined from oxygen  $2p_\sigma$  orbitals, see Ref. [11], but these states do not contribute to the effect and we neglect them. In the work [11] the wave functions (4) have been matched to the gadolinium  $6s$  and  $6p$

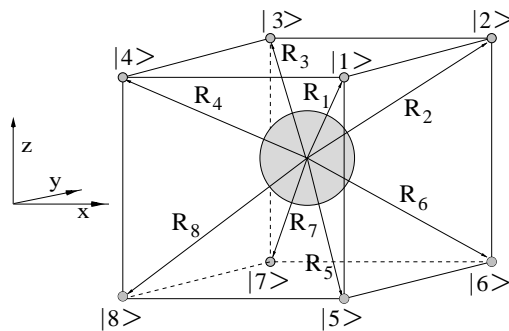


FIG. 2:  $Gd^{3+}$  ion with surrounding eight oxygen ions.

wave functions at the matching sphere of radius  $R \approx 2.5a_B$  around Gd. This is a simple and reliable way to describe penetration of oxygen electrons inside  $Gd^{3+}$ . However, unfortunately this is not a consistent quantum mechanical description because the space is divided in two parts — inside and outside of the matching sphere. Our analysis has shown that calculation of exchange diagrams in this simple model is ambiguous. The point is that the effect arises in the third order of perturbation theory (see below). In such a high order one must use a consistent quantum mechanical description. The best solution of the problem would be a 3-dimensional Hartree-Fock or 3-dimensional pseudo-potential calculation for the cluster consisting of Gd and eight oxygen ions (GdO<sup>8</sup>-cluster). However this is a very complex calculation. In the present work we suggest an intermediate solution, essentially a jelly model. We assume that eight oxygen ions provide a spherically symmetric attractive potential for electrons

$$V_O(\mathbf{r}) = -A_o e^{-\left(\frac{r-r_o}{D}\right)^2} \tag{5}$$

where  $r_o = 4.53$  is Gd-O distance, and  $A_o$  and  $D$  are some parameters. So effectively we replace the dodecahedron in Fig. 1 or the cube in Fig. 2 by a sphere. Thus the electrons are moving in the combined spherically symmetric potential

$$V(\mathbf{r}) = V_{Gd}(\mathbf{r}) + V_O(\mathbf{r}), \tag{6}$$

where  $V_{Gd}$  is the potential of  $Gd^{3+}$  core (2), and  $V_O$  is the combined potential of oxygens (5). Solution of the Dirac equation with potential (6) gives single particle orbitals. In this picture the electronic configuration of the GdO<sup>8</sup>-cluster is  $1s^2 \dots 5s^2 5p^6 4f^7 6s^2 6p^6$ . Out of this  $1s^2 \dots 5s^2 5p^6 4f^7$  are the  $Gd^{3+}$  electrons and  $6s^2 6p^6$  are in essence the oxygen electrons. So we have eight oxygen electrons, this is exactly what one needs to describe S and P  $2p_\sigma$  states (4). In this model one cannot describe D and F states combined from  $2p_\sigma$  oxygen orbitals, but fortunately there is no need in these states because they do not contribute to the effect.

How to determine the constants  $A_o$  and  $D$  in the effective oxygen “jelly” potential (5)? The size of the potential  $D$  is not very important, it is clear that  $D \sim 1$  (we remind that we use atomic units), and we set  $D = 1$ . The depth of the potential  $A_o$  is crucially important. Wave functions of oxygen ion  $O^{2-}$  have been calculated in Ref. [17], so  $\psi_{2p_\sigma}$

is known. We chose the depth  $A_o$  from the requirement that the wave functions  $\psi_{6s}$  and  $\psi_{6p}$  satisfy the following conditions

$$\begin{aligned} |\psi_{6s}(R)| &= |\psi_{2p_\sigma}(r_o - R, \cos\theta = 1)|, \\ |\psi_{6p}(R, \cos\theta = 1/\sqrt{3})| &= |\psi_{2p_\sigma}(r_o - R, \cos\theta = 1)|, \end{aligned} \quad (7)$$

where  $R \approx 2.5$ . This is just an alternative formulation of the idea of dual description at  $r \approx R$ , see Refs. [11, 17]. There are two conditions (7) and only one parameter  $A_o$ , so strictly speaking one cannot satisfy both conditions exactly. However at  $A_o = 0.9$  each of the conditions (7) is satisfied with accuracy  $\sim 15\%$ , and this is the value of  $A_o$  which we use in our calculations. Thus, parameters of the ‘‘oxygen’’ potential (5) are

$$r_o = 4.53, \quad A_o = 0.9, \quad D = 1. \quad (8)$$

Let  $f(r)$  be the upper component of the Dirac spinor,  $\psi(r) = f(r)/r \cdot Y_{lm}(\theta, \phi)$ . The electron density  $|f(r)|^2$  for  $6s$ ,  $6p_{1/2}$ , and  $6p_{3/2}$  states calculated in the potential (6) is shown in Fig. 3. The density is peaked at  $r = r_o = 4.53$ ,

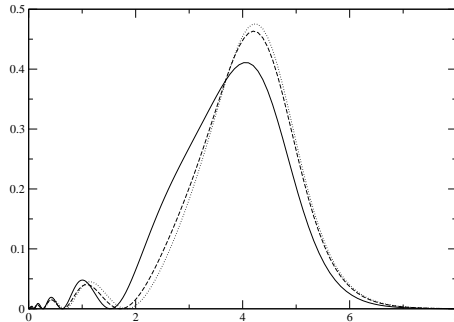


FIG. 3: Radial electron density  $|f(r)|^2$ ,  $\psi(r) = f(r)/r \cdot Y_{lm}(\theta, \phi)$ , versus distance from the Gd nucleus. The solid line corresponds to the  $6s$ -state, the dashed line corresponds to the  $6p_{1/2}$ -state, and the dotted line corresponds to the  $6p_{3/2}$ -state.

this is the effective description of oxygen ions. Energies of  $4f$ ,  $5d$ ,  $6s$ , and  $6p$  states in the potential (6) are listed in Table II. The energies are given with respect to the ionization limit. It is worth to note that according to this

State	$4f_{5/2}$	$4f_{7/2}$	$5d_{3/2}$	$5d_{5/2}$	$6s$	$6p_{1/2}$	$6p_{3/2}$
Energy	-366	-360	-299	-295	-311	-289	-286

TABLE II: Energy levels in the potential (6) with respect to the ionization limit. Units  $10^3 \text{ cm}^{-1}$ .

calculation the  $5d$ - $4f$  splitting is  $\Delta E_{fd} \approx 66 \times 10^3 \text{ cm}^{-1}$ . This is different from the splitting for an isolated  $\text{Gd}^{3+}$  ion,  $\Delta E_{fd} \approx 100 \times 10^3 \text{ cm}^{-1}$ , see Ref. [13]. However, the value  $\Delta E_{fd} \approx 66 \times 10^3 \text{ cm}^{-1}$  agrees well with that extrapolated for the  $\text{Gd}^{3+}$  ion in the garnet environment, see Ref. [18].

### III. T,P-ODD ENERGY CORRECTION RELATED TO THE LATTICE DEFORMATION

Similar to the approach [11] in this section we consider an external deformation of the lattice consisting in a shift of the  $\text{Gd}^{3+}$  ion with respect to surrounding oxygen ions. Later we will relate the deformation to observable effects.

We have already mentioned the T,P-odd effect arises in the third order of perturbation theory. So, there are three perturbation theory operators we have to consider. First of all this is the operator of the T,P-odd interaction of the electron EDM  $d_e$  with atomic electric field  $\mathbf{E}$ , see e.g. Ref. [5],

$$V_d = -d_e \gamma_o \boldsymbol{\Sigma} \cdot \mathbf{E}. \quad (9)$$

Here  $\gamma_o$  and  $\boldsymbol{\Sigma} = \gamma_o \gamma_5 \boldsymbol{\gamma}$  are Dirac  $\gamma$ -matrices. Because of the Schiff’s theorem [19] it is crucial to account for complex many-body screening effects, when working with the Hamiltonian (9). Technically this means that the many-body perturbation theory with operator (9) is very poorly convergent. The standard way [5] to avoid this complication is to

split the Hamiltonian (9) into two terms:  $V_d = -d_e \gamma_o \boldsymbol{\Sigma} \cdot \mathbf{E} = -d_e \boldsymbol{\Sigma} \cdot \mathbf{E} - d_e (\gamma_o - 1) \boldsymbol{\Sigma} \cdot \mathbf{E}$ . Then due to the Schiff's theorem contribution of the first term to an observable effect is identically zero, so one can reduce the interaction

$$V_d \rightarrow V_d^r = -d_e (\gamma_o - 1) \boldsymbol{\Sigma} \cdot \mathbf{E}. \quad (10)$$

The perturbation theory expansion with this operator is reasonably convergent.

The second perturbation operator is related to the shift of the  $\text{Gd}^{3+}$  ion with respect to the surrounding oxygen ions. Let us denote value of the shift by  $x$ . In our model, this corresponds to the shift of spherically symmetric  $V_O(r)$  (5) along one of the axes, say  $z$ -axis, see Fig. 4

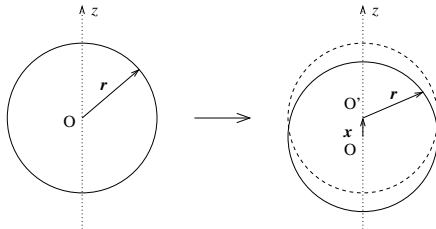


FIG. 4: Schematic picture, illustrating the shift of  $V_O(\mathbf{r})$  due to the lattice deformation.

Therefore

$$V_O(\mathbf{r}) \rightarrow V_O'(\mathbf{r}) = V_O(\mathbf{r} + \mathbf{x}) = V_O(\mathbf{r}) + \frac{(\mathbf{x} \cdot \mathbf{r})}{r} \frac{\partial V_O}{\partial r} = V_O(\mathbf{r}) + x \cos \theta \frac{\partial V_O}{\partial r}. \quad (11)$$

We keep the term linear in  $x$ ,  $\theta$  is the azimuthal angle. Thus the perturbation operator related to the lattice deformation reads

$$V_x(r) = x \cos \theta \frac{\partial V_O}{\partial r} = -2x \cos \theta \frac{(r - r_o)}{D^2} V_O(r) \quad (12)$$

The third perturbation operator is residual electron-electron Coulomb interaction, which is not included in the effective potential

$$V_C(\mathbf{r}_i, \mathbf{r}_j) = \frac{1}{|\mathbf{r}_i - \mathbf{r}_j|} = \sum_{lm} \frac{4\pi}{2l+1} \frac{r_{<}^l}{r_{>}^{l+1}} Y_{lm}^*(\mathbf{r}_i) Y_{lm}(\mathbf{r}_j) \quad (13)$$

Here  $\mathbf{r}_i$  and  $\mathbf{r}_j$  are radius-vectors of interacting electrons.

Formula for the energy correction in the third order of perturbation theory reads, see e.g. Ref. [20]

$$E_n^{(3)} = \sum_m' \sum_k' \frac{V_{nm} V_{mk} V_{kn}}{\hbar^2 \omega_{mn} \omega_{kn}} - V_{nn} \sum_m' \frac{|V_{nm}|^2}{\hbar^2 \omega_{nm}^2}, \quad (14)$$

where

$$V = V_d^r + V_x + V_C. \quad (15)$$

In Eq. (14) we need to consider only the terms that are linear in each of the operators  $V_d^r$  (10),  $V_x$  (12), and  $V_C$  (13). There are 15 diagrams corresponding to Eq. (14), these diagrams are presented in Fig. 5. Each diagram contributes with a coefficient shown before the diagram. Summation over *all* intermediate states  $|k\rangle$  and  $|m\rangle$  and over *all filled* states  $|n\rangle$  is assumed. The first four are the direct diagrams that correspond to the mechanism considered in [11]. All other diagrams are exchange ones and therefore they contribute with sign  $(-)$ . This is not so with respect to the disconnected exchange diagrams with brackets. These contributions correspond to the negative term in (14). In the exchange diagrams we account only for  $s$ - $p$  mixing by  $V_d^r$ , contributions of higher angular momenta are neglected, see e.g. Ref. [5]. The deformation (dashed line) is also attached only to  $s$ - $p$  lines because it is practically saturated by  $6s$ - and  $6p$ -states. Since  $V_d^r$  and  $V_x$  are single particle operators we evaluate each diagram solving equations for corresponding corrections. For example the first diagram contains on the right top leg the correction

$$\delta\psi_x = \sum_m \frac{\langle mp_{1/2} | V_x | ns \rangle}{\epsilon_{ns} - \epsilon_{mp_{1/2}}} | mp_{1/2} \rangle. \quad (16)$$

To evaluate the correction we do not use a direct summation, but instead solve the equation

$$(H - \epsilon)\delta\psi_x = -V_x|ns\rangle, \quad \epsilon = \epsilon_{ns} \quad (17)$$

for each particular  $|ns\rangle$  state. Here  $H$  is the Dirac Hamiltonian with potential (6). Similarly the bottom left leg of the diagram 5 is evaluated using

$$(H - \epsilon_{ns})\delta\psi_d = -V_d^T|ns\rangle \quad (18)$$

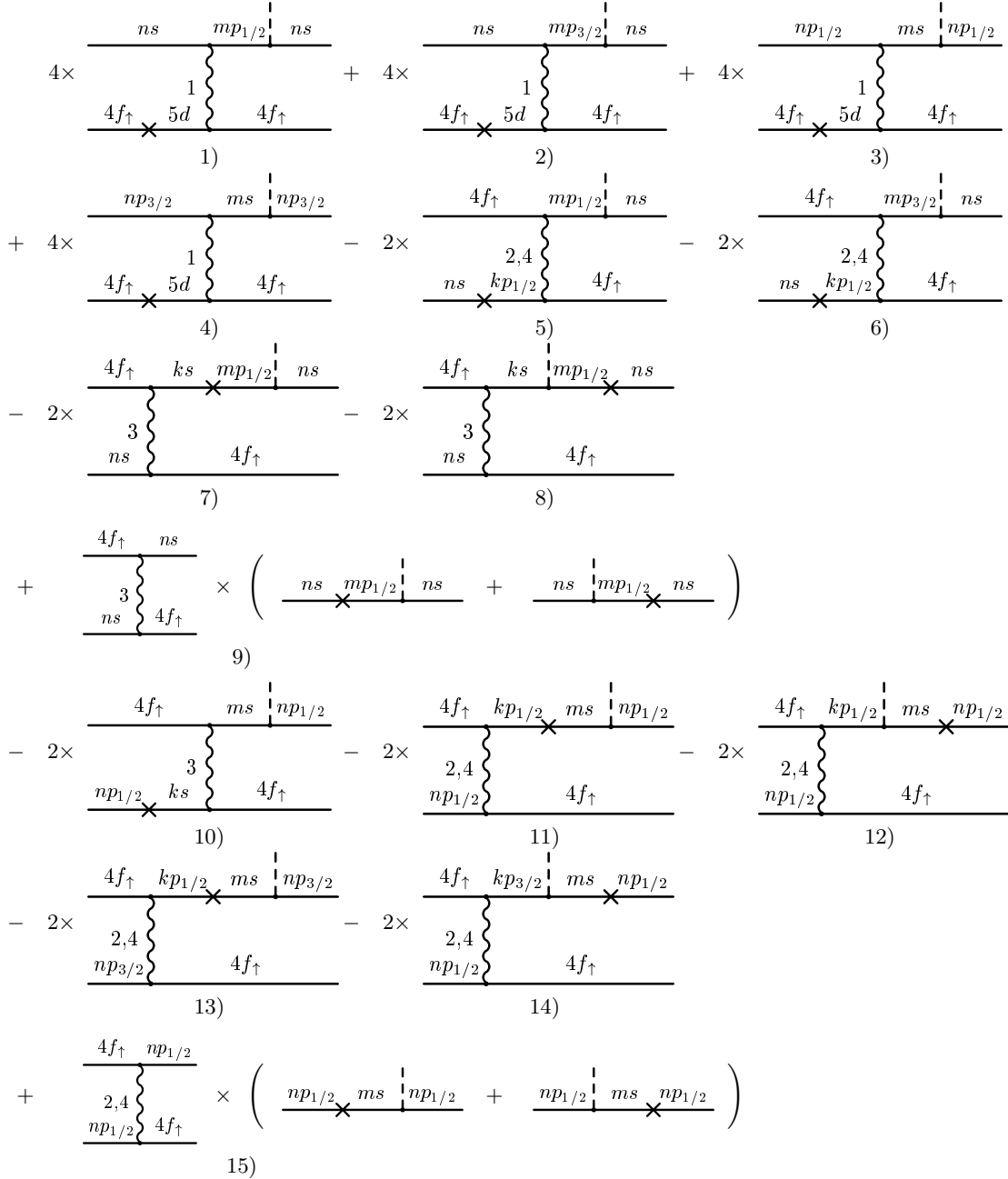


FIG. 5: Third order perturbation theory diagrams corresponding to Eq. (14). The cross denotes the T,P-odd interaction  $V_d^T$  (10), the dashed line denotes the lattice deformation perturbation  $V_x$  (12), and the wave line denotes the Coulomb interaction  $V_C$  (13). Multipolarity of the Coulomb interaction is shown near the line. Each diagram contributes with a coefficient shown before the diagram. Summation over *all* intermediate states  $|k\rangle$  and  $|m\rangle$  and over *all filled* states  $|n\rangle$  is assumed.

Diagrams with two single particle operators on the leg require a more careful treatment. For example to evaluate the

top right leg of the diagram 7 we first find  $\delta\psi_x$  using Eq. (17). After that we calculate  $\delta\psi_{dx}$  using

$$(H - \epsilon_{ns})\delta\psi_{dx} = -V_d^T \delta\psi_x + \langle ns|V_d^T|\delta\psi_x\rangle|ns\rangle. \quad (19)$$

The additional term  $\langle ns|V_d^T|\delta\psi_x\rangle|ns\rangle$  in the right hand side of the equation is due to the orthogonality condition  $\langle \delta\psi_{dx}|ns\rangle = 0$ . The corrections  $\delta\psi_{dx}$  in diagrams 13 and 14 clearly do not require any additional terms in the corresponding equations. Finally the disconnected diagrams (diagrams with brackets) which originate from the second term in (14) contain the energy denominator squared. For example the bracket in the diagram 9 is equal to  $2\langle ns|V_d^T|\delta\phi_x\rangle$  where

$$\delta\phi_x = \sum_m \frac{\langle mp_{1/2}|V_x|ns\rangle}{(\epsilon_{ns} - \epsilon_{mp_{1/2}})^2} |mp_{1/2}\rangle. \quad (20)$$

To find  $\delta\phi_x$  we calculate  $\delta\psi_x$  at  $\epsilon = \epsilon_{ns} \pm \delta$ , see Eq. (17), and then find  $\delta\phi_x$  using numerical differentiation

$$\delta\phi_x = - \left. \frac{\delta\psi_x(\epsilon_{ns} + \delta) - \delta\psi_x(\epsilon_{ns} - \delta)}{2\delta} \right|_{\delta \rightarrow 0}. \quad (21)$$

As a result of the calculations we get the following T,P-odd energy correction related to the displacement  $x$

$$\begin{aligned} \Delta\epsilon(x) &= -A \frac{x}{a_B} \left( \frac{d_e}{ea_B} \right) E_0 (\mathbf{n}_S \cdot \mathbf{n}_x), \\ A &= -0.094 - 0.159 + 0.080 + 0.133 + 0.141 - 0.295 - 0.257 \\ &\quad - 0.040 + 0.610 - 0.295 - 0.009 - 0.001 + 0.440 - 0.159 \\ &= 0.095. \end{aligned} \quad (22)$$

We remind that  $a_B$  is the Bohr radius, and  $e = |e|$  is the elementary charge, so the ratio of the electron EDM  $d_e$  to  $ea_B$  is dimensionless. The results in (22) is given in atomic units,  $E_0 = 27.2eV$ . The unit vectors are  $\mathbf{n}_S = \mathbf{S}/S$ ,  $\mathbf{n}_x = \mathbf{x}/x$ , where  $S = 7/2$  is spin of Gd ion. Fourteen terms in  $A$  represent contributions of fifteen diagrams Fig. 5. For diagrams 13 and 14 we present only the combined contribution (+0.440). The point is that each of these two diagrams gives a very large contribution inversely proportional to the fine structure splitting. However these large contributions are canceled out in the sum of 13 and 14, so the sum remains finite even at zero fine structure splitting. For this reason we do not calculate 13 and 14 separately.

#### IV. T,P-ODD VOLTAGE ACROSS MAGNETICALLY POLARIZED SAMPLE OF GDIG, AND MAGNETIZATION OF GGG IN THE EXTERNAL ELECTRIC FIELD

In a magnetically polarized sample, according to Eq. (22), each  $Gd^{3+}$  ion can gain energy from a small distortion of the lattice. The lattice has some stiffness and therefore the variation of energy per Gd ion as a function of the displacement  $x$  is of the form

$$\Delta\epsilon(x) = \frac{1}{2}Kx^2 - A \frac{x}{a_B} \frac{d_e}{ea_B} E_0, \quad (23)$$

where  $K$  is the effective elastic constant per  $Gd^{3+}$  ion. Minimum value of  $\Delta\epsilon(x)$  corresponds to the shift

$$\frac{x}{a_B} = A \frac{E_0}{Ka_B^2} \frac{d_e}{ea_B}, \quad (24)$$

which is the new equilibrium position of  $Gd^{3+}$  in the magnetically polarized sample.

To find  $x$  one needs to know  $K$ . In Ref. [11] value of this constant has been estimated using the known static dielectric constant of GdIG  $\epsilon \approx 15$  and using a rather simplistic picture of the dielectric polarization. In the present work we estimate  $K$  using analysis of data on infrared spectroscopy of garnets [21, 22]. According to [21, 22] the so called ‘‘N’’ and the ‘‘O’’ infrared modes are related to movement of Gd. The N mode in GdIG has energy  $\omega_N = 213cm^{-1}$ . Energy of the O mode is unfortunately unknown. However similar modes are known in Yttrium iron garnet:  $\omega_N = 208.8cm^{-1}$ ,  $\omega_O = 144cm^{-1}$ . Assuming the same ratio  $\omega_N/\omega_O$  we find for GdIG:  $\omega_O = 147cm^{-1}$ . Movement of Gd is not a normal mode of the lattice, however the splitting between  $\omega_N$  and  $\omega_O$  is not large. Therefore to find the effective frequency we average between the modes

$$\omega = \frac{1}{2}(\omega_N + \omega_O) = 180cm^{-1}. \quad (25)$$

The elastic constant is equal to

$$K = \mu\omega^2, \quad (26)$$

where  $\mu$  is the reduced mass corresponding to movement of Gd with respect to the lattice of the garnet  $\text{Gd}_3\text{Fe}_5\text{O}_{12}$ ,

$$\frac{1}{\mu} = \frac{1}{M_{\text{Gd}}} + \frac{3}{5M_{\text{Fe}} + 12M_{\text{O}}}, \quad \rightarrow \quad \mu = 77. \quad (27)$$

Together with (25) and (26) this gives

$$K = 0.095 \frac{E_0}{a_B^2}. \quad (28)$$

Accidentally the dimensionless coefficient in this equation is the same as that in Eq. (22). The value (28) is by factor 2.35 smaller than that obtained in Ref. [11] from the dielectric constant. We believe that the present analysis is more reliable and gives the more accurate value of the elastic constant. Further analysis of the lattice vibrations and a new data on the infrared absorption would be very helpful for precise determination of the elastic constant.

Using Eqs. (24) and (28) we obtain the value of the displacement induced by the electron EDM,  $x \approx d_e/e$ . Macroscopic electric polarization arising from the shift of Gd ions in the sample is given by  $P = 3exn_{\text{Gd}}$ , where  $n_{\text{Gd}} = 1.235 \times 10^{22} \text{ cm}^{-3}$  is number density of Gd in GdIG. Hence, the electric field in the sample is

$$E = -4\pi P \approx 12\pi n_{\text{Gd}} d_e = -1.1 \times 10^{-10} \text{ V/cm}. \quad (29)$$

The numerical value corresponds to the current upper limit on the electron EDM (1). For a 10cm sample this gives a voltage  $\Delta V = 1.1 \times 10^{-9} \text{ V}$ . This value is a factor 3 greater than that obtained in [11]. The difference is mainly due to the different elastic constant.

Another effect is magnetization in the external electric field. A candidate for such experiment is gadolinium gallium garnet (GGG), see Ref. [7]. There is no need to repeat the calculation [11], we need only to rescale the value. According to the present work the value of  $A$  in Eq. (22) is a factor 1.27 larger than that from [11] and the elastic constant is a factor 2.35 smaller than that from [11] (we assume that the elastic constants for GdIG and GGG coincide). Therefore, the energy shift of  $\text{Gd}^{3+}$  ion in GGG in the external electric field is

$$\Delta\epsilon = (\mathbf{n}_E \cdot \mathbf{n}_S) 5.7 \times 10^{-22} \text{ eV}, \quad (30)$$

where  $\mathbf{n}_E$  is the unit vector along the electric field, and  $\mathbf{n}_S$  is the unit vector along the ion spin. The value corresponds to the current upper limit on  $d_e$  (1) and the electric field inside the sample  $E = 10 \text{ kV/cm}$ . The energy shift (30) leads to the macroscopic magnetization of the sample. The magnetization depends also on temperature and internal magnetic interactions in the compound. We do not discuss these points here. According to estimates [7] the magnetization due to the energy shift  $\sim 10^{-22} \text{ eV}$  can be measured and moreover the prospects for improvement of sensitivity are very good.

## V. CONCLUSIONS

In the present work we have calculated the T,P-odd effects induced by the electron electric dipole moment (EDM) in gadolinium gallium garnet,  $\text{Gd}_3\text{Ga}_5\text{O}_{12}$  (GGG), and gadolinium iron garnet  $\text{Gd}_3\text{Fe}_5\text{O}_{12}$  (GdIG). Both GdIG and GGG have uncompensated electron spins on  $\text{Gd}^{3+}$  ions. There are two possibilities to probe the electron EDM. The first one is to polarize magnetically the electron spins and to measure the induced voltage across the sample. According to the present calculation at the current limitation on the electron EDM, (1), the induced voltage across a 10cm sample is  $1.1 \times 10^{-9} \text{ V}$ . Another possibility is to apply an electric field to the unpolarized sample. This leads to the spin-dependent energy shift of each Gd ion  $\Delta\epsilon = 5.7 \times 10^{-22} \text{ eV}$  at  $E = 10 \text{ kV/cm}$ . This can be measured via macroscopic magnetization of the sample.

In the present work we generally followed the path of [11]. However the electronic part of the problem has been considered much more accurately with account of exchange diagrams which have been neglected in [11]. Surprisingly, because of accidental compensations, the final electronic effective Hamiltonian proved to be close to that from [11]. Nevertheless the observable effects are by 3 times bigger than that in [11]. The main reason for this is in the different lattice elastic constant. To determine value of the constant in the present work we have used data on infrared absorption of garnets. A new data on the infrared absorption and further analysis of the lattice vibrations would be very helpful for more accurate calculations of observable effects. However the main problem which bothers us



is the electronic part. In the present work we have used a “jelly model” smearing eight oxygen ions surrounding gadolinium ion over a spherical shell. It is a sensible simplification. However we found strong compensations between contributions of different exchange diagrams. Clearly the compensations are related to the Schiff theorem. In this situation any simplification causes questions and, in our opinion, a further calculation of the effect with account of real 3D geometry is necessary.

- 
- [1] J. H. Christensen, J. W. Cronin, V. L. Fitch, and R. Turlay, *Phys. Rev. Lett.* **13**, 138 (1964).
  - [2] A. D. Sakharov, *Sov. Phys. JETP Lett.* **5**, 24 (1967).
  - [3] J. Schwinger, *Phys. Rev.* **91**, 720, 723 (1953); W. Pauli in *Niels Bohr and the Development of Physics* (Pergamon Press, London, 1955).
  - [4] A. Angelopoulos *et al*, *Phys. Lett. B* **444**, 43 (1998).
  - [5] I. B. Khriplovich and S. K. Lamoreaux, *CP Violation Without Strangeness* (Springer, Berlin, 1997).
  - [6] B. C. Regan, E. D. Commins, C. J. Schmidt, and D. DeMille, *Phys. Rev. Lett.* **88**, 071805 (2002).
  - [7] S. K. Lamoreaux, *Phys. Rev. A* **66**, 022109 (2002).
  - [8] L. R. Hunter, Talk at the workshop *Tests of Fundamental Symmetries in Atoms and Molecules*, Harvard, 2001. Available online <http://itamp.harvard.edu/fundamentalworkshop.html>
  - [9] F. L. Shapiro, *Usp. Fiz. Nauk* **95**, 145 (1968) [*Sov. Phys. Usp.* **11**, 345 (1968)].
  - [10] B. V. Vasil'ev and E. V. Kolycheva, *ZhETF* **74**, 466 (1978) [*Sov. Phys. JETP* **47**, 243 (1978)].
  - [11] S. Kuenzi, O. P. Sushkov, V. A. Dzuba and J. M. Cadogan, *Phys. Rev. A* **66**, 032111 (2002).
  - [12] S. Y. Buhmann, V. A. Dzuba, and O. P. Sushkov, *Phys. Rev. A* **66**, 042109 (2002).
  - [13] V. A. Dzuba, O. P. Sushkov, W. R. Johnson, and U. I. Safronova, *Phys. Rev. A* **66**, 032105 (2002).
  - [14] O. P. Sushkov, V. V. Flambaum, and I. B. Khriplovich, *Zh. Eksp. Teor. Fiz.* **87**, 1521 (1984) [*Sov. Phys. JETP* **60**, 873 (1984)]
  - [15] W. C. Martin, R. Zalubas and L. Hagan, *Atomic Energy Levels - The Rare-Earth Elements* (NSRDS-NBS 60, 1978).
  - [16] *Physics of Magnetic Garnets*, ed A. Paoletti, North-Holland, Amsterdam, 1978.
  - [17] V. V. Flambaum and O. P. Sushkov, *Physica C* **168**, 565, (1990).
  - [18] P. Dorenbos, *Journal of Luminescence* **91**, 91 (2000).
  - [19] L. I. Schiff, *Phys. Rev.* **132**, 2194 (1963).
  - [20] L. D. Landau and E. M. Lifshitz, *Quantum Mechanics: Non-Relativistic Theory* (Pergamon, 1977).
  - [21] A. M. Hofmeister and K. R. Campbell, *J. Appl. Phys.* **72**, 638 (1992).
  - [22] R. Moretti and G. Ottonello, *Geochimica et Cosmochimica Acta* **62**, No 7, 1147 (1998)